Available online at www.sciencedirect.com
ScienceDirect
Sensors and Actuators A 136 (2007) 510–517
SENSORS AND ACTUATORS A PHYSICAL
www.elsevier.com/locate/sna

Carbon nanotube micropatterns and cantilever arrays fabricated with layer-by-layer nano self-assembly

Wei Xue, Tianhong Cui *

Mechanical Engineering and Nanofabrication Center, University of Minnesota, 111 Church Street S.E., Minneapolis, MN 55455, United States

Received 23 June 2006; received in revised form 3 October 2006; accepted 5 October 2006
Available online 2 November 2006

Abstract

The two-dimensional (2D) microstructures and three-dimensional (3D) cantilever arrays based on single-walled carbon nanotube (SWNT) multilayer were fabricated by combining electrostatic layer-by-layer (LbL) nano self-assembly, microlithography, and lift-off. The combinative technique provides a simple, effective, low-cost, and low-temperature fabrication method with a short processing time. The 2D SWNT micropatterns with a feature size of 5 μm were fabricated and characterized. The thickness of a (PDDA/SWNT) bi-layer was measured approximately as 76 Å. SWNTs were randomly deposited on the substrate, and they were interconnected and formed as a dense network. To investigate the potential applications of SWNTs, magnetic cantilever arrays formed with SWNTs, iron oxide (Fe_2O_3) nanoparticles, and polyelectrolytes were developed. A modified lift-off process was developed to provide additional protection for the cantilever arrays. Due to the outstanding mechanical properties of the SWNTs, the fabricated cantilevers are very strong and highly flexible. The cantilever arrays can be used in applications such as biosensors and microvalves.

Keywords: Single-walled carbon nanotube (SWNT); Multilayer; Layer-by-layer (LbL) nano self-assembly; Lithography; Lift-off

1. Introduction

Since the discovery in 1991, carbon nanotubes (CNTs) have been investigated extensively due to their unique structural, electrical, chemical, and mechanical properties [1]. CNTs can be seen as nanoscale cylinders rolled up by graphene sheets. The bonding structure between carbon atoms of CNTs is sp^2 bond, which is stronger than the sp^3 bond found in diamond. Therefore, CNTs have outstanding mechanical strength with an estimated Young's modulus greater than 1 TPa [2]. Depending on the diameter and chirality, CNTs can be either metallic or semiconducting [3]. Both types of CNTs can serve as key components for nanoscale devices. In their natural forms, CNTs are highly sensitive to molecules such as NO_2 and NH_3 [4]. With rational chemical and/or physical modification, CNTs are capable of detecting many types of molecules (e.g., H_2, CO, glucose, and DNA) [5]. Ever since their discovery, CNTs have been explored and used in a wide range of applications including chemical sensors, biosensors, stress/strain sensors, scanning probes, field emission displays, nanoelectromechanical systems (NEMS), and nanoelectronic devices [6–10]. However, currently most CNT-based devices are still far from commercialization. One of the biggest problems for producing practical CNT devices is how to precisely deposit CNTs on the substrate. The controllable deposition of CNTs, either individually or as a bulk material, is an essential step to build practical devices.

Current controllable deposition approaches include chemical vapor deposition (CVD), selective electrophoresis deposition, Langmuir–Blodgett method, and manipulation using atomic force microscope tips [11,12]. However, these techniques require long deposition time, complicated procedures, and expensive instruments. One recent experiment incorporated direct deposition of organic molecules by dip-pen nanolithography and large-scale assembly of (CNTs) [13]. A number of monolayer microstructures were fabricated on a gold surface with this method. However, this technique can only be used on substrates with a layer of Au, and can only be used to deposit a monolayer. To overcome these limitations, electrostatic layer-by-layer (LbL) nano self-assembly was introduced to produce multilayer films in micro- and nanoscale. LbL nano self-

* Corresponding author. Tel.: +1 612 626 1636; fax: +1 612 625 6069.
E-mail address: tcui@me.umn.edu (T. Cui).

0924-4247/$ – see front matter © 2006 Elsevier B.V. All rights reserved.
doi:10.1016/j.sna.2006.10.006

assembly is an effective and economic approach to build well-organized multilayers in nanometer scale. LbL self-assembled thin films can be deposited on the surface of almost any materials with any topography [14]. With this technique, CNT thin films have been fabricated and investigated by several groups. Compared with other CNT/polymer matrices, LbL self-assembled CNT thin films show enhanced mechanical properties. These films have Young's modulus of 17–35 GPa [15]. In addition, the thin films fabricated with LbL self-assembly usually retain the electrochemical catalytic activities of the CNTs [16].

In this paper, we report a simple, effective, and versatile technique to fabricate the two- and three-dimensional (2D and 3D) microstructures based on single-walled carbon nanotube (SWNT) multilayer. This technique combines the "bottom–up" LbL nano assembly and the "top–down" microlithography technique. It provides a simple, low-cost, and low-temperature fabrication method with a short processing time. The SWNT multilayer films and 2D micropatterns were built with alternating layers of poly(dimethyldiallylammonium chloride) (PDDA) and SWNTs. The randomly assembled SWNTs were interconnected and formed a dense network on the substrate. The assembled multilayer film was characterized. The enhanced mechanical properties of SWNT thin films can be utilized in a variety of applications. To investigate the potential applications of SWNT thin films, magnetic cantilever arrays composed of PDDA, SWNTs, and iron oxide (Fe_2O_3) nanoparticles were fabricated. Multi-step ultraviolet (UV) lithography and photoresist development were combined with LbL self-assembly to produce the 3D cantilever arrays. A modified lift-off technique was used to provide additional protection for the cantilever arrays.

2. Self-assembly and material preparation

Among all types of nanofabrication techniques, LbL nano self-assembly has attracted much attention due to its versatility and simplicity. It can overcome the size limitation of the current "top–down" lithography-based microfabrication techniques. Ultrathin films can be built through alternate adsorption of oppositely charged species such as polyelectrolytes, nanoparticles, SWNTs, and proteins [17]. The species are held together by strong ionic bonds, and form uniform and stable thin films. The scheme of LbL self-assembly of polyelectrolytes, SWNTs, and Fe_2O_3 nanoparticles is illustrated in Fig. 1. By repeating the adsorption steps, a multilayer with precisely controlled thickness can be obtained. With a proper (positive–negative–positive) alternation, the SWNTs and Fe_2O_3 nanoparticles can be assembled in any order.

The polyelectrolytes, including PDDA (polycation, molecular weight MW 200,000–350,000, 15 mg/ml) and poly(sodium 4-styrenesulfonate) (PSS, polyanion, MW 70,000, 3 mg/ml) were obtained from Sigma–Aldrich. In order to increase the ionic strength and enhance the adsorption of the polyions, 0.5 M NaCl was added to both polyelectrolyte solutions. Magnetic iron oxide nanoparticles (Fe_2O_3, 50 nm in diameter, surface covered with hydrophilic PSS, concentration: 2 mg/ml) were obtained from Chemicell GmbH. The Fe_2O_3 nanoparticles are negatively

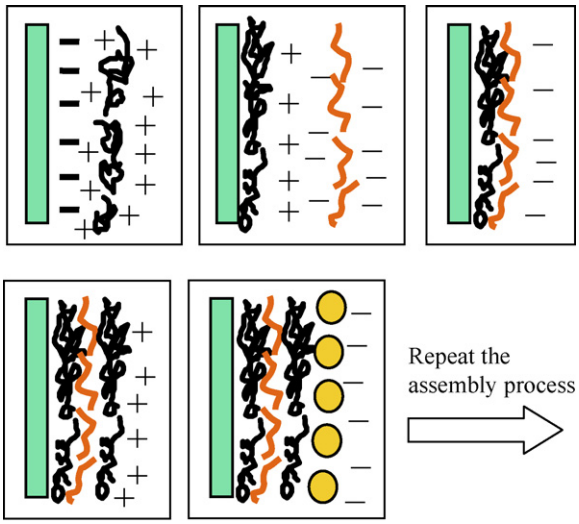

Fig. 1. Scheme of layer-by-layer nano self-assembly of polycation/SWNTs and polycation/Fe_2O_3 nanoparticles. The oppositely charged species are bonded together based on electrostatic forces. The repeating of the assembly process can form uniform and stable thin films.

charged due to the surface coverage of PSS. All materials were diluted in deionized (DI) water. Pristine SWNTs (powder, 1.1 nm in diameter, 50 μm in length, density of 2.1 g/cm^3, purity > 90%) were purchased from Chengdu Organic Chemicals Co. Ltd.

Due to their exceptional mechanical properties, SWNTs can be used to mix with other polymers to produce strong mechanical composites. However, it is well known that pristine SWNTs suffer from poor solubility in most solvents. The hybrid polymer/SWNT composites made by mixing often have problems such as poor polymer-SWNT connectivity, phase segregation, and structural inhomogeneities [15]. LbL self-assembly is a good approach to overcome these problems because it is a solution-based technique. SWNTs with rational treatment can be dispersed in DI water, and uniformly deposited on the substrate. Highly homogenous polymer/SWNT thin films with enhanced mechanical properties can be fabricated. In order to increase the solubility and processability of SWNTs, defects such as terminal groups can be intentionally introduced to their sidewalls and open ends [18]. The chemical oxidation method is chosen to process the pristine SWNTs. The SWNTs were chemically functionalized by a mixture of nitric and sulfuric acid (1:3 HNO_3:H_2SO_4) at 110 °C for 45 min. The mixture of acids cut the SWNTs into short tubes with openings at both ends. Carboxylic (–COOH) functional groups were covalently attached to the open ends and sidewalls. Next, the SWNT dispersion was diluted with DI water and filtered with a PVDF membrane (with a pore diameter of 0.22 μm) which has excellent acid resistance. The SWNTs were then rinsed with DI water to remove the residual acids. The treated SWNTs were dispersed in DI water and ultrasonically vibrated for 1 h. The final step was to remove the excessive SWNTs by centrifuging the SWNT dispersion at 5000 rpm for 15 min. After the chemical funcationalization, the SWNTs were negatively charged and uniformly dispersed in DI water with a concentration of 1 mg/ml.

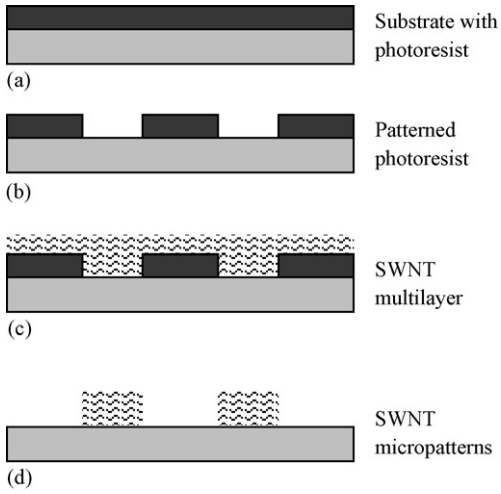

Fig. 2. Fabrication process of the SWNT micropatterns by (a) spin coating, (b) lithography, (c) LbL nano self-assembly, and (d) lift-off.

3. Experiments

3.1. Two-dimensional SWNT micropatterns

We reported a lithographic technique to pattern nanoparticle-based thin films previously [19,20]. Complex and distinct structures of the multilayer films were produced with a combinative technique, including LbL self-assembly, lithography, and lift-off. The same approach can be used to pattern SWNT thin films. We have successfully fabricated microscale patterns on both silicon and polymer substrates with this approach. The process and the generated 2D structures are almost identical for both substrates. In this paper, we focus on the fabrication and micropatterns on silicon substrates.

The fabrication process to produce 2D SWNT micropatterns is shown in Fig. 2. First, a layer of positive photoresist (PR1813, 1.5 μm thick) is spin coated on a 4-in. silicon wafer (Fig. 2a). Second, the wafer is exposed under UV light to transfer the patterns from the chrome photomask to the photoresist. After exposure, the photoresist is developed with MF351 developer for 30 s (Fig. 2b). Third, the SWNT multilayer is deposited on the substrate with LbL self-assembly (Fig. 2c). The substrate is soaked in different solutions, and the sequence of the immersion is: [PDDA (10 min) + PSS (10 min)]$_2$ + [PDDA (10 min) + SWNTs (15 min)]$_n$, where n represents the number of (PDDA/SWNT) bi-layers. The coating of the first two (PDDA/PSS) bi-layers works as the precursor layer. It increases the charge strength of the silicon substrate, and prepares a smooth base for the subsequent coating. Intermediate rinsing with DI water and drying with a nitrogen flow are required to remove the excessive polyelectrolytes and SWNTs. The final step is to dissolve the photoresist and remove the SWNT multilayer with lift-off technique (Fig. 2d). The substrate is soaked in acetone for 1 min with the assistance of ultrasonic vibration. The self-assembled SWNT multilayer is permeable for acetone. Acetone molecules can penetrate through the SWNT thin film, dissolve the photoresist, and strip off the SWNT multilayer from those areas. Only the SWNT multilayer directly assembled on the substrate remains. The fabricated SWNT micropatterns were inspected by scanning electron microscopy (SEM, JEOL 6500). Fig. 3 shows the SEM images of micro-springs with a linewidth of 5 μm (Fig. 3a) and assembled SWNTs on the substrate (Fig. 3b). The samples used for microscopy inspection are (PDDA/SWNT)$_6$ micropatterns. The SWNT multilayer thin film is formed by a dense network of SWNTs. The SWNTs are randomly deposited on the surface. The length of the SWNTs is in the range of 1–2 μm after the chemical treatment. However, as shown in the figure, the diameters of most SWNTs are much larger than pristine SWNTs (1.1 nm). The reason for this discrepancy is that during the self-assembly process, several SWNTs are wrapped together due to their extremely high aspect ratios. Therefore, the assembled SWNTs are mainly in the form of nanotube bundles, which are approximately 5–10 nm in diameter and 1–2 μm in length.

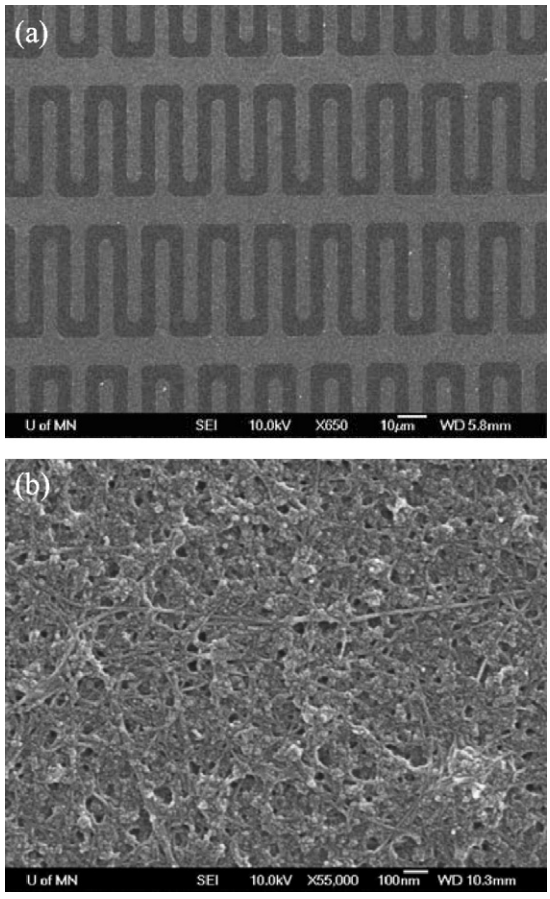

Fig. 3. (a) SEM image of (PDDA/SWNT)$_6$ micro-springs with linewidth of 5 μm. (b) Close SEM inspection of assembled SWNTs on the substrate.

In the assembly process, the SWNTs are coated on the substrate in a repeated fashion. The multilayer can be considered as several accumulated (PDDA/SWNT) bi-layers. To estimate the thickness of the SWNT multilayer, a group of micro-lines (with linewidth of 50 μm) was fabricated on a silicon substrate using the method described above. The micro-lines are composed of six (PDDA/SWNT) bi-layers. They were characterized both

mechanically and optically. Surface profiler (Dektak, Model IIA) was used to mechanically measure the vertical profile of the SWNT lines. The average thickness of the $(PDDA/SWNT)_6$ structure was measured approximately as 400 Å. The surface profiler obtains its measurement data by moving a diamond tip stylus over the patterns during the scan. It usually gives relatively accurate results on hard substrates. However, when used on soft thin films, the scanning is destructive and may give inaccurate results (often smaller than the actual values). In order to verify the results from the surface profiler measurement, an ellipsometer (Gaertner Scientific Co.) was used to optically detect the thin film thickness. Ellipsometer provides a non-destructive method and gives more accurate results once the rough thickness of the film is known. The measured thickness of the $(PDDA/SWNT)_6$ multilayer from the ellipsometer measurement was $455.4 \pm 5\%$ Å. Therefore, the average thickness of a (PDDA/SWNT) bi-layer is approximately 75.9 Å.

Quartz crystal microbalance (QCM, Maxtek RQCM) was used to monitor the growth of the SWNT multilayer. The quartz crystal resonator (AT cut, 9 MHz resonant frequency, 1 in. in diameter) used in the measurement was covered with Au electrodes on both sides. The QCM equipment is an extremely sensitive microbalance capable of detecting mass changes in ng/cm^2 range. It also provides a real-time measurement of quartz crystal frequency and frequency shift. Therefore, the saturation time for adsorbing polyelectrolytes, SWNTs, and nanoparticles can be estimated. During the adsorption, the crystal was held vertically in the solutions to avoid excessive coating of materials. The crystal was immersed in PDDA and SWNT solutions for given periods of time. The real-time frequency shift of the crystal was recorded by the QCM. The mass change ΔM (g) and the frequency shift Δf(Hz) can be expressed by Sauerbrey equation [21]:

$$\Delta f = -C_f \times \Delta m = -C_f \times \frac{\Delta M}{A} \quad (1)$$

$$d = -\frac{\Delta f}{\rho \cdot C_f} \quad (2)$$

where $C_f = 1.81 \times 10^8$ (Hz cm^2/ng) is the sensitivity factor of the 9 MHz AT cut crystal, Δm (g/cm^2) is the change in mass per unit area, $A = 0.34$ cm^2 is the active oscillation region of the crystal which is limited to the overlapping area of the front and rear Au electrodes, d is the layer thickness, and ρ is the density of the deposited material, $\rho_{PDDA} = 1.2$ g/cm^3 and $\rho_{SWNT} = 2.1$ g/cm^3.

Fig. 4 shows the growth of a $(PDDA/SWNT)_6$ multilayer monitored with QCM. The left y-axis shows the frequency shift Δf recorded by QCM and the right y-axis illustrates the calculated layer thickness. The average frequency changes of PDDA and SWNTs are −61.1 and −182.5 Hz, respectively. Based on Eq. (2), the average layer thicknesses calculated for PDDA and SWNT are $d_{PDDA} = 2.8$ nm and $d_{SWNT} = 4.8$ nm, respectively. Therefore, the thickness of a (PDDA/SWNT) bi-layer is approximately 7.6 nm, which is very close to the value obtained with ellipsometer.

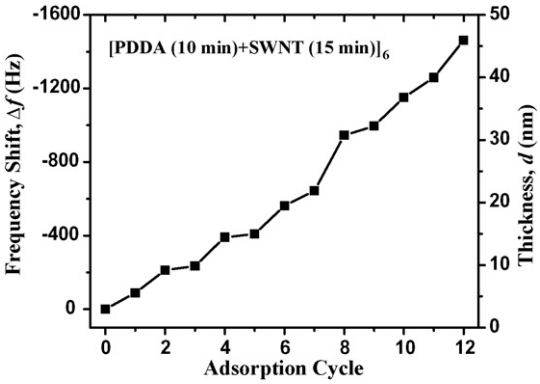

Fig. 4. Growth of a $(PDDA/SWNT)_6$ multilayer monitored with QCM.

3.2. Three-dimensional SWNT magnetic cantilever arrays

One of the most important advantages of SWNTs is their high mechanical strength. The SWNTs are capable of increasing the mechanical strength of other materials when SWNTs are incorporated. The mechanical properties of the LbL self-assembled SWNT thin film were studied and reported. The Young's modulus of the SWNT film was measured as 17–35 GPa, and the ultimate tensile strength was measured as 180–325 MPa [15]. Compared with strong polymers, which are commonly used for MEMS devices such as polymethyl methacrylate (PMMA, Young's modulus: 2 GPa, ultimate tensile strength: 50 MPa), SWNT thin films are several times stronger. SWNT films also have enough flexibility due to its composite essence. With proper adjustments, the SWNT films may achieve a wide range of mechanical properties between silicon and polymers. The SWNT thin films can serve as structural components in MEMS devices to provide both flexibility and strength. In addition, the "bottom–up" LbL self-assembly technique has the ability to control the film thickness in nanometer scale. Therefore, the SWNT films can provide structural platforms with highly adjustable mechanical properties, and have the potential to be used in a variety of applications.

To investigate the potential applications of SWNT multilayer thin films, 3D SWNT-based magnetic cantilever arrays composed of PDDA, SWNTs, and Fe_2O_3 nanoparticles were designed and fabricated. The schematic diagram of the SWNT cantilever array is illustrated in Fig. 5. Both the roots and the beams are composed of SWNT multilayer. Fe_2O_3 nanoparticles are integrated in the multilayer as magnetically sensitive mate-

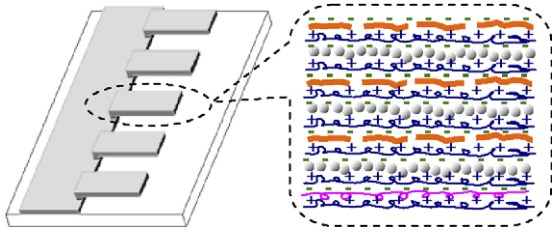

Fig. 5. Scheme diagram of the cantilever array fabricated on silicon substrate. The enlarged area illustrates the multilayer which consists of PDDA (+), PSS (−), Fe_2O_3 nanoparticles (−), and SWNTs (−).

rial, which makes the actuation and measurement convenient. The cantilever array can be used in detecting biomolecules such as proteins, enzymes, and DNAs. A number of biomolecules are naturally charged, and can be assembled in alternation with polyelectrolytes based on LbL self-assembly technique. Because the cantilevers are self-assembled multilayer thin films, the surfaces of the cantilevers are charged. The biomolecules can be readily adsorbed onto the cantilevers. The resonant frequency shift caused by the mass increase of the cantilever can be detected by an optical interferometer. Another possible application is to use the cantilever beams as magnetically driven microvalves.

Surface coverage is a factor frequently used to describe the self-assembly of spherical nanoparticles. It is defined as the ratio of the estimated layer thickness and the diameter of the nanoparticle. If the substrate is totally covered by the nanoparticles, as shown in Fig. 6a, the surface coverage is 100%. The scheme shown in Fig. 6b has a surface coverage of 50%. However, it is difficult to obtain the accurate surface coverage by visual inspection of the assembled nanoparticle multilayers. QCM provides a more accurate method to estimate the surface coverage by measuring the mass increase of the crystal. Research shows that the self-assembled nanoparticles are hexagonally packed (Fig. 6c). The volume ratio of the nanoparticles in the assembled multilayer is approximately 60% [22]. The other 40% are air-filled pores, which are excluded from the QCM thickness calculation. Therefore, the surface coverage r of the spherical nanoparticles can be expressed as:

$$r = \frac{d/60\%}{d_s} = \frac{1}{60\%} \cdot \frac{d}{d_s} = \frac{1}{60\%} \cdot r_e \tag{3}$$

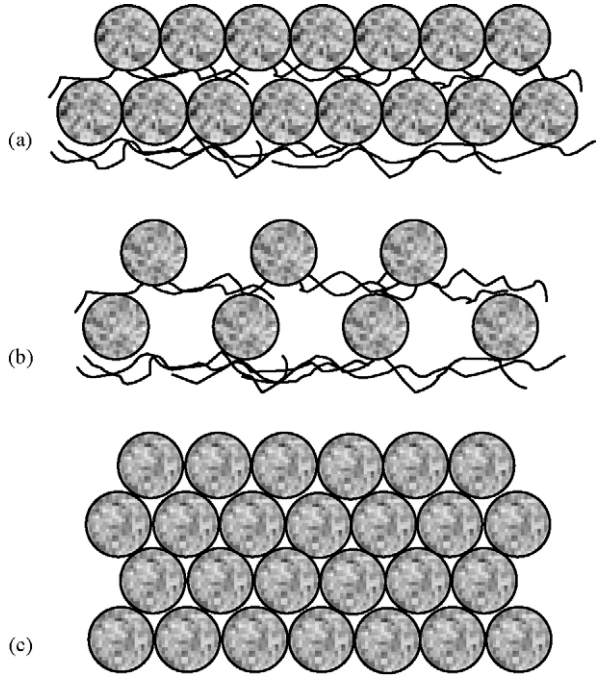

Fig. 6. Schematic representation of self-assembled nanoparticles: (a) side view of close-packed nanoparticles, (b) side-view of sparse-packed nanoparticles, and (c) top-view of hexagonal close-packed nanoparticles.

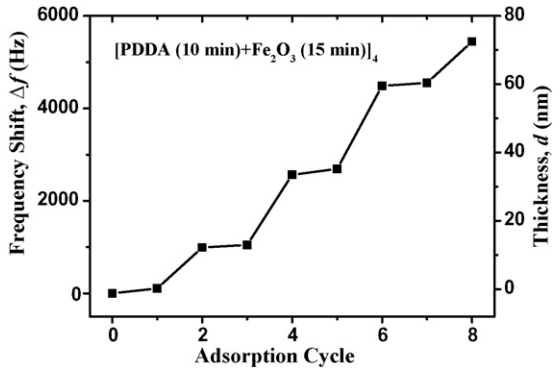

Fig. 7. Growth of a $(PDDA/Fe_2O_3)_4$ multilayer monitored with QCM.

where d is layer thickness from Eq. (2), d_s is the diameter of the nanoparticle, and r_e is the effective surface coverage. Fig. 7 shows the growth of a $(PDDA/Fe_2O_3)_4$ multilayer monitored with QCM. The average frequency shift of the Fe_2O_3 nanopar-

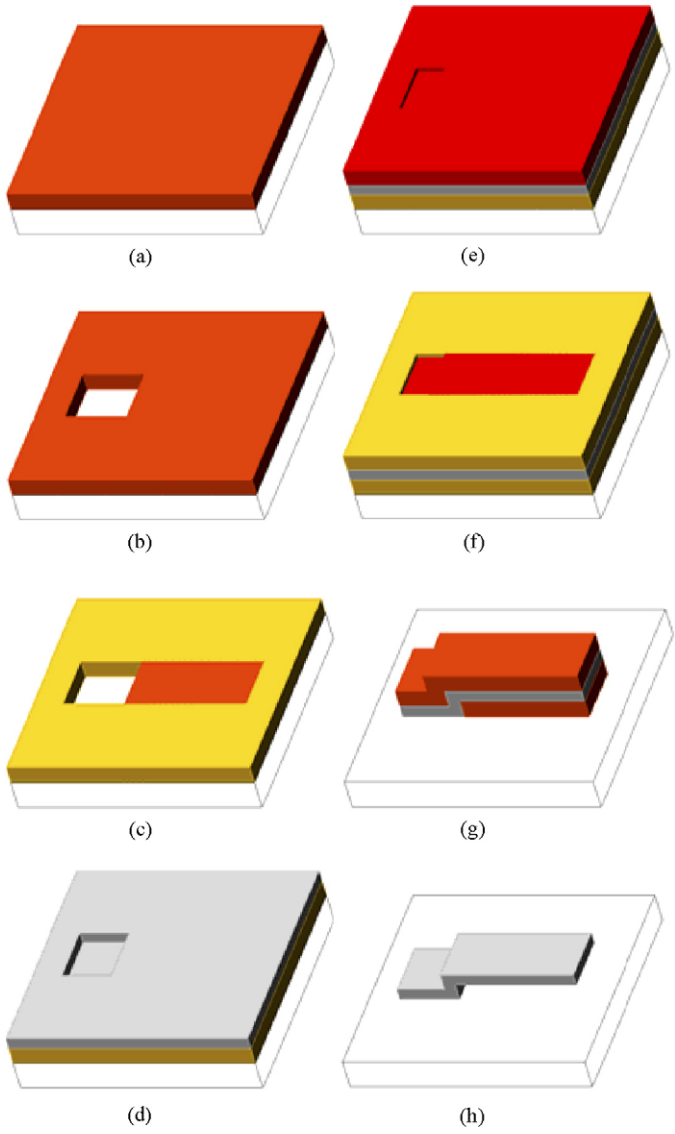

Fig. 8. (a–h) Fabrication process of the self-assembled cantilever with modified lift-off technique.

ticle adsorption is approximately −1273.4 Hz. Based on Eq. (2), the average thickness of the Fe_2O_3 nanoparticle layer is 13.4 nm. The effective surface coverage of the nanoparticles is estimated as $r_e = d/d_s = 13.4\,\text{nm}/50\,\text{nm} = 26.8\%$. Therefore, the surface coverage r can be calculated as 44.7% from Eq. (3). The relatively low surface coverage can be increased by using Fe_2O_3 suspensions with higher concentrations.

The fabrication of 3D cantilever arrays is based on the 2D patterning technique. The process includes several UV lithography and photoresist development steps. A modified lift-off technique is used to provide addition protection for the cantilevers [23]. The fabrication process of the 3D cantilever is shown in Fig. 8. The figure only shows the fabrication of one cantilever for simplicity and clarity, the array can be produced with the same process. A layer of photoresist PR1813 is spin coated on the substrate (Fig. 8a). The first UV lithography and development are used to open a window for the cantilever root (Fig. 8b). The second UV lithography is executed with part of the PR1813 layer protected. The protected PR1813 is used as the sacrificial layer underneath the cantilever beam (Fig. 8c). The PDDA/PSS/SWNT/Fe_2O_3 multilayer is self-assembled on the substrate (Fig. 8d). The immersion sequence is [PDDA (10 min) + PSS (10 min)]$_2$ + {PDDA (10 min) + Fe_2O_3 (15 min) + [PDDA (10 min) + SWNTs (15 min)]$_2$ + PDDA (10 min) + Fe_2O_3 (15 min) + PDDA (10 min) + SWNTs (15 min)}$_3$. Nine layers of SWNTs are used to strengthen the cantilever structure. Six layers of Fe_2O_3 nanoparticles make the cantilever magnetically sensitive. Another layer of PR1813 is spin coated on the substrate and covers the assembled multilayer (Fig. 8e). The third lithography is executed. The part of the photoresist that covers the cantilever root and beam is protected by photomask, while the other part of the photoresist is exposed under UV light (Fig. 8f). The exposed PR1813 is dissolved with MF351 developer. In order to remove the multilayer coated on the exposed PR1813, this step is implemented with ultrasonic vibration (Fig. 8g). As a result, the unexposed PR1813 layers and the cantilever in between remain on the substrate. The freestanding cantilever beam is released by stripping off the PR1813, the bottom sacrificial layer and the top protection layer, with acetone (Fig. 8h). Based on the QCM measurement, the effective thickness of the whole multilayer can be calculated approximately as 200 nm.

The modified lift-off process is illustrated in Fig. 8e–g. Compared with the standard lift-off technique, it has a top photoresist layer in addition to the bottom sacrificial layer. Moreover, the stripper used in the modified process is photoresist developer instead of commonly used acetone. The micropatterns fabricated with standard lift-off processes usually have step profiles. The stripper molecules can easily attack the underlying photoresist layer and remove the unwanted top layer. However, as shown in Fig. 8d, the self-assembled multilayer covers the whole surface of the device, and is almost at the same height. To form the

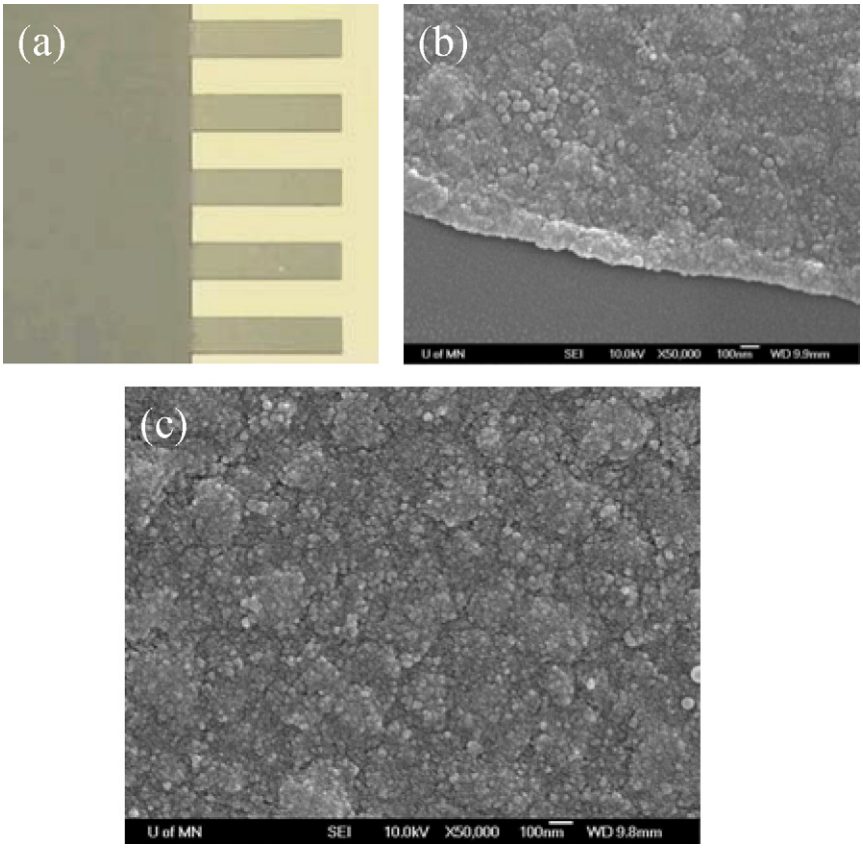

Fig. 9. Images of the LbL self-assembled cantilever array. (a) Optical image of the cantilever array. The length and the width of the beams are 200 and 50 μm, respectively. (b) SEM inspection of the edge of the cantilever. (c) SEM image of the assembled Fe_2O_3 nanoparticles.

cantilever structure, ultrasonic vibration is required to break the multilayer. With the standard lift-off, it takes 8–10 min for ultrasonic vibration to break the multilayer and remove the unwanted part of the thin film due to its high mechanical strength. The long-time ultrasonic bath severely weakens and damages the cantilever structure, especially the joint between the root and the beam. The weakening of the structure may cause detachment of the beam from the root. The modified technique involves a "sandwich" structure, which provides additional protection for the cantilever. Based on the modified lift-off process, the ultrasonic bath time can be greatly reduced to 2 min. Both the cantilever root and beam are well protected by the top photoresist layer.

Cantilever arrays with different dimensions were fabricated with the combinative technique described above. The images of the fabricated cantilever array are shown in Fig. 9. Fig. 9a shows an optical image of a cantilever consists of five beams. The length and width of these beams are 200 and 50 μm, respectively. Fig. 9b shows a close SEM inspection of the edge of the beam and Fig. 9c shows the assembled Fe_2O_3 nanoparticles on the surface of the cantilever. The sparsely deposited Fe_2O_3 nanoparticles can be seen from the images. To strip off the top protecting and the bottom sacrificial photoresist layers, the device is submerged in acetone. An external magnetic field is applied by holding a permanent magnet (with a magnetic field strength of 0.02 T) at 1 cm above the device. The magnetic field strength applied on the cantilever array is approximately 0.005 T. Fig. 10 illustrates the cantilever beam behavior during the magnetic actuation. The cantilever beam is gradually deflected from 0° to about 135°. The beam restores rapidly after moving the magnetic away from the device. There is no observable structural failure or damage after repeated deflections (more than 100 times). The SWNT multilayer is proven to be very flexible and strong, which are preferred properties of cantilever-based biosensors. However, the internal stress inside the SWNT multilayer is not neglectable. In a number of cases, the free ends of the cantilever beams are curled in the acetone solution. This may cause measurement problems if optical interferometry method is used. Further studies will be conducted to solve the problem. Possible solutions include increasing the multilayer thickness, trimming the corners of the beams, increasing the number of SWNT layers, etc.

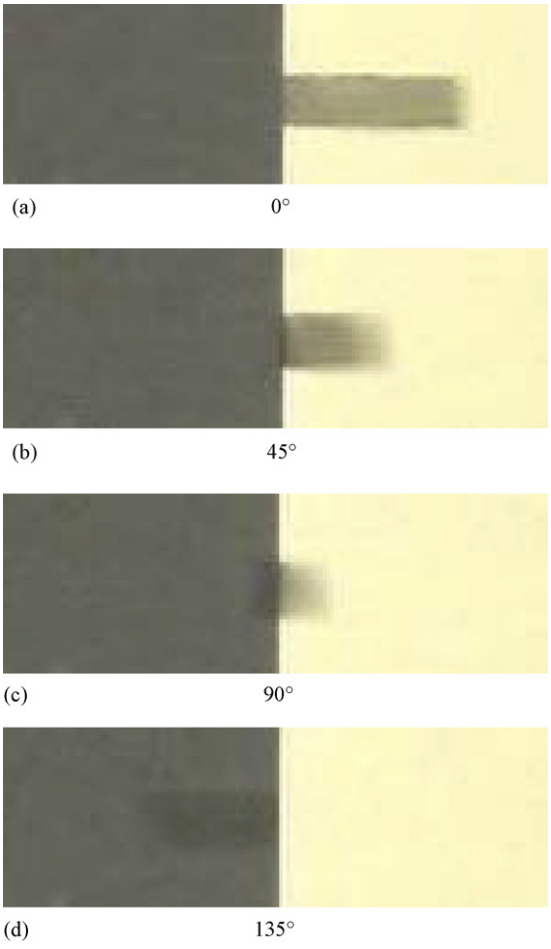

Fig. 10. Flexed cantilever in acetone with an external magnetic field. Four optical images illustrate the deflection of a cantilever at four different angles: (a) 0°, (b) 45°, (c) 90°, and (d) 135°.

4. Conclusion

We have presented an effective, simple, low-cost, and low-temperature approach to fabricate SWNT multilayer thin films, 2D micropatterns, and 3D cantilever arrays by combining LbL nano self-assembly and microlithography. SWNT micropatterns with a feature of 5 μm have been produced. It is believed that the patterned feature size can be downscaled to submicron or even nanoscale if high-resolution lithography techniques such as electron-beam lithography are used. The thickness of a (PDDA/SWNT) bi-layer is approximately 76 Å. Magnetic cantilever arrays composed of polyions/SWNTs/Fe_2O_3 nanoparticles have been fabricated based on self-assembled multilayer thin films. A modified lift-off process has been developed to provide additional protection for the cantilever structures. The strength and thickness of the cantilevers can be adjusted in a wide range. The cantilevers are very flexible and highly strong; they can be easily deflected to over 90°. The fabricated cantilever arrays can be used as magnetically driven microactuators. They can also be used in biosensing applications such as biomolecule adsorption and detection because a number of biomolecules can be easily adsorbed on the self-assembled multilayer.

References

[1] S. Iijima, Helical microtubules of graphitic carbon, Nature 354 (1991) 56.
[2] C.N.R. Rao, B.C. Satishkumar, A. Govindaraj, M. Nath, Nanotubes, Chemphyschem 2 (2001) 78–105.
[3] T. Dürkop, B.M. Kim, M.S. Fuhrer, Properties and applications of high-mobility semiconducting nanotubes, J. Phys. Condens. Mat. 16 (2005) R553–R580.
[4] J. Kong, N.R. Franklin, C. Zhou, M.G. Chapline, S. Peng, K. Cho, H. Dai, Nanotube molecular wires as chemical sensors, Science 287 (2000) 622–625.
[5] J. Kong, M.G. Chapline, H. Dai, Functionalized carbon nanotubes for molecular hydrogen sensors, Adv. Mater. 13 (2001) 1384–1386.
[6] R.H. Baughman, C. Cui, A.A. Zakhidov, Z. Lqbal, J.N. Barisci, G.M. Spinks, G.G. Wallace, A. Mazzoldi, D. De Rossi, A.G. Rinzler, O. Jaschinski, S. Roth, M. Kertesz, Carbon nanotube actuators, Science 284 (1999) 1340–1344.

[7] S.J. Tans, A.R.M. Verschueren, C. Dekker, Room-temperature transistor based on a single carbon nanotube, Nature 393 (1998) 49–52.
[8] K.A. Williams, P.T.M. Veenhuizen, B.G. de la Torre, R. Eritja, C. Dekker, Carbon nanotubes with DNA recognition, Nature 420 (2002) 761.
[9] W.B. Choi, D.S. Chung, J.H. Kang, H.Y. Kim, Y.W. Jin, I.T. Han, Y.H. Lee, J.E. Jung, N.S. Lee, G.S. Park, J.M. Kim, Fully sealed, high-brightness carbon-nanotube field-emission display, Appl. Phys. Lett. 75 (1999) 3129–3131.
[10] M. Penza, F. Antolini, M.V. Antisari, Carbon nanotubes as SAW chemical sensors materials, Sens. Actuators B 100 (2004) 47–59.
[11] L. Valentini, C. Catalini, I. Armentano, J.M. Kenny, L. Lozzi, S. Santucci, Highly sensitive andselective sensors based on carbon nanotubes thin films for molecular detection, Diam. Relat. Mater. 13 (2004) 1301–1305.
[12] Y. Jang, S. Moon, J. Ahn, Y. Lee, B. Ju, A simple approach in fabricating chemical sensor using laterally grown multi-walled carbon nanotubes, Sens. Actuators B 99 (2004) 118–122.
[13] S.G. Rao, L. Huang, W. Setyawan, S. Hong, Large-scale assembly of carbon nanotubes, Nature 425 (2003) 36–37.
[14] Y. Xia, G.M. Whitesides, Soft lithography, Annu. Rev. Mater. Sci. 28 (1998) 153–184.
[15] A.A. Mamedov, N.A. Kotov, M. Prato, D.M. Guldi, J.P. Wicksted, A. Hirsch, Molecular design of strong single-wall carbon nanotube/polyelectrolyte multilayer composites, Nat. Mater. 1 (2001) 190–194.
[16] M. Zhang, K. Gong, H. Zhang, L. Mao, Layer-by-layer assembled carbon nanotubes for selective determine of dopamine in the presence of ascorbic acid, Biosens. Bioelectron. 20 (2005) 1270–1276.
[17] G. Decher, Fuzzy nanoassemblies: toward layered polymeric multicomposites, Science 277 (1997) 1232–1237.
[18] S. Banerjee, T. Hemraj-Benny, S.S. Wong, Covalent surface chemistry of single-walled carbon nanotubes, Adv. Mater. 17 (2005) 17–29.
[19] F. Hua, J. Shi, Y. Lvov, T. Cui, Patterning of layer-by-layer self-assembled multiple types of nanoparticle thin films by lithographic technique, Nano Lett. 2 (2002) 1219–1222.
[20] F. Hua, T. Cui, Y. Lvov, Ultrathin cantilevers based on polymer-ceramic nanocomposite assembled through layer-by-layer adsorption, Nano Lett. 4 (2004) 823–825.
[21] G. Sauerbrey, Use of crystal oscillators for weighing thin films and for micro weighing, Zeitschrift fur Physik 155 (1959) 206–222.
[22] Y. Lvov, K. Ariga, M. Onda, I. Ichinose, T. Kunitake, Alternate assembly of ordered multilayers of SiO_2 and other nanoparticles and polyions, Langmuir 13 (1997) 6195–6203.
[23] W. Xue, T. Cui, Single-walled carbon nanotube micropatterns and cantilever array fabricated with electrostatic layer-by-layer nano self-assembly and lithography, in: Tech. Digest, Solid-State Sensor, Actuator and Microsystems Workshop, Hilton Head Island, SC, USA, June 4–8, 2006, pp. 328–331.

Biographies

Wei Xue received the BS degree and the MS degree in electrical engineering from Shandong University in 1997 and 2000, respectively. He is currently pursuing his PhD degree at Department of Mechanical Engineering, University of Minnesota. His main research interest includes microfabrication techniques, nanotechnology, polymer/silicon microelectromechanical systems (MEMS), micro/nano electronics, chemical and biological sensors, modeling, and system control.

Tianhong Cui received the BS degree from Nanjing University of Aeronautics and Astronautics in 1991, and the Ph.D. degree from the Chinese Academy of Sciences in 1995.

He is currently a Nelson associate professor of Mechanical Engineering at the University of Minnesota. From 1999 to 2003, he was an assistant professor of electrical engineering at Louisiana Technical University. Prior to that, he was a STA fellow at National Laboratory of Metrology, and served as a postdoctoral research associate at the University of Minnesota and Tsinghua University. He received research awards including the Nelson Endowed Chair Professorship from the University of Minnesota, the Research Foundation Award from Louisiana Tech University, the Alexander von Humboldt Award in Germany, and the STA & NEDO fellowships in Japan. He is a senior member of IEEE and a member of ASME. His current research interests include MEMS/NEMS, nanotechnology, and polymer electronics.